Human Thermoregulation and Spatial Temperature for Frostbite Prediction with Bio-Heat Transfer Model

Juliette Jacques[1,2], Timothy Rioux[1], Xiaojiang Xu[1], John Castellani[1]

[1] United States Army Research Institute of Environmental Medicine
[2] Oak Ridge Institute for Science and Education (ORISE)

Abstract

The following work outlines the male and female finite element thermoregulatory models (FETM) for frostbite prediction with COMSOL Multiphysics Software using the bio-heat transfer module[1, 2]. The models use medical phantoms of the median U.S. male and female to provide an anatomically accurate geometric mesh, including layers of skin, fat, muscle, bones, and 9 essential organs. Using a variable order Backward Differentiation Formula (BDF) during Time-Dependent simulations, the models predict the spatial temperature distribution across all layers at high resolution. Models were previously validated with thermoneutral, hot and cold conditions. In this paper, we evaluate the models in extreme cold and windy conditions for the prediction of exposure time to frostbite. Simulations are compared to the current National Weather Service (NWS) Wind Chill Temperature Index (WCTI) and published data in similar conditions [3]. In the male and female FETM, the results show shorter exposure times to frostbite in the finger and nose compared to the cheek. Male and female FETM results are compared, with an observed difference in the finger times to frostbite.

Keywords: Bio-heat transfer, spatial temperature, thermoregulation, frostbite, wind chill temperature

Introduction

Frostbite and cold injury risk in below freezing ambient air temperature (T_{air}) is exacerbated by wind, ultimately increasing the time to frostbite with increasing wind velocities (v_{wind}). The combined cooling effect of low temperatures and wind is called wind chill temperature. Wind chill models have primarily utilized numerical methods and cylindrical models in predicting frostbite risk in humans (Appendix 1). The current National Weather Service (NWS) Wind Chill Temperature Index (WCTI) [3], calculates skin temperatures for frostbite risk on the cheek with minimal activity levels based on heat exchange models not considerate of protective clothing, exercise, or sex differences. However, areas other than the cheek pose a greater threat of accelerated times to frostbite due to factors of reduced blood flow, larger surface area to mass proportion or limited clothing thermal resistance. Regions of higher susceptibility than the cheek include the nose and fingers. Therefore, a more accurate WCTI should consider additional body regions, thermal clothing, sex, and various metabolic rates. These considerations are applied in the following male and female thermoregulatory models in COMSOL Multiphysics to determine the exposure duration until frostbite, given specific conditions. From previous work, it was expected that the nose and 5th finger will reach frostbite at an accelerated rate compared to the cheek; furthermore, increased metabolic rates would increase time to frostbite in all regions. Based on the areas of interest, we expect that the male and female model predictions would not be significantly different.

Theory

Active System

Humans possess the ability to stabilize internal temperature as ambient conditions vary. This temperature regulation is enacted by thermoreceptor signals, and carried out with several physiological responses including vasoconstriction, vasodilation, sweating, and shivering heat production. Afferent signals dependent on environmental conditions are sent to the brain to provide necessary information to the central nervous system for the appropriate responses. Efferent signals are then responsible for sending signals from the brain to the peripheral nervous system to initiate action, in this case physiological response. In hot temperatures vasodilation occurs, the process of dilating blood vessels and maximizing blood flow to the surface. Sweating is another cooling response to allow for

evaporative heat loss from the body. In cold ambient conditions, vasoconstriction is invoked to reduce blood vessel size and blood flow to the surface (skin, fat, muscle) to allow for more blood flow to essential internal organs. Shivering is another response invoked to create more metabolic heat production and warm the body in cold conditions. This will be referred to as the *active system.*

Passive System

Thermal energy transfer in the in the human body relies on geometry, anatomical characteristics, and thermal properties of organs and tissues. In the following models, heat exchange occurs between tissues and blood, in the respiratory tract and the skin surface to environment boundary. A central blood pool is assumed in which venous blood and surrounding tissues reach an equilibrium temperature. Mechanisms of heat transfer on the skin boundary include conduction, convection, radiation, and evaporation. In respiratory heat exchange, this consists of convective and evaporative transfer. Both sites rely on total metabolic heat production, ambient temperature, and vapor pressure. The mentioned heat transfer components in the human body are considered the *passive system.*

Simulation Methods

Male and female thermoregulatory models were developed using Extended Cardiac-Torso (XCAT) images of median U.S. adults, segmented with Simpleware™ Scan IP workflow from voxelized data to a CAD model and the final tetrahedral meshes (Appendix 2) were imported into COMSOL Multiphysics software with 6.2 million tetrahedral elements [1, 2]. The male model represents the median U.S. adult male at 37 years old, 1.76 m tall and 81kg; the female model is representative of the median U.S. adult female at 36 years old, 1.62 m tall and 66kg. Male and female meshes were segmented into 13 tissues and organs, including the skin, fat, muscles, bones, eyes, liver, stomach, lungs, heart, kidneys, bladder, intestines, and brain (Figure 1 & 2).

The imported mesh components were designated with attributes for thermoregulation, including thermal resistivity, conductivity, specific heat capacity and initial temperature conditions. The models used COMSOL's Bio-Heat Transfer module to implement the passive system components. Spatial temperature distribution on the surface is determined by the bio-heat transfer equation (passive system) [Eq.1] and efferent system responses for thermoregulation by error signals from the hypothalamus (active system) [Eq.5,6].

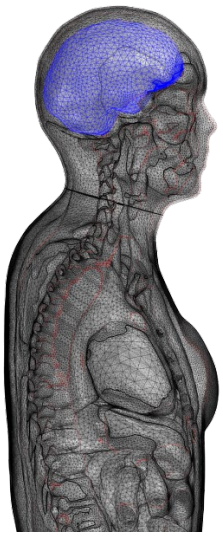

Figure 1: Cut plane of female mesh with segmented brain (purple)

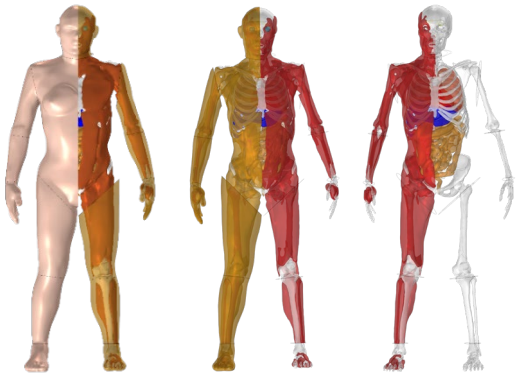

Figure 2: Skin layer and fat layer [Left], fat layer and muscle layer [Middle], muscle layer and bones and organs [Right]

The bio-heat transfer equation describing heat balance in the body is:

$$\rho C_p \frac{\partial T}{\partial t} = \lambda \nabla^2 T + Q_0 + Q_{SH} + Q_{EX} + \beta \omega \rho_b C_{p,b}(T_b - T) \quad \text{[Eq.1]}$$

where ρ is the density, C_p represents specific heat, T is the temperature, t is time, λ is thermal conductivity, Q_0 is basal metabolic heat production, Q_{SH} and Q_{EX} are shivering and exercise heat production, β is the countercurrent heat exchange factor, ω is blood flow rate, ρ_b is blood flow rate, $C_{p,b}$ is specific heat of blood, and T_b is the temperature of blood. The assumed central blood pool was added as a global equation in COMSOL as the following heat balance equation, where V_b is the volume of blood:

$$V_b \rho_b C_{p,b} \frac{dT_b}{dt} = \beta \omega \rho_b C_{p,b} (T - T_b) dV \qquad \text{[Eq.2]}$$

In both models, the initial temperature of blood is 37℃. On the skin surface, the boundary equation without clothing is:

$$-\lambda \frac{\partial T}{\partial n} = (h_c + h_r) \cdot (T_s - T_o) + E \qquad \text{[Eq.3]}$$

where h_c and h_r are the convection and radiation coefficients, respectively, T_s is surface temperature, T_o is operative temperature (defined by Castellani et. al) and E is evaporative heat loss by sweating.

Clothing resistance is considered in the same layer as the skin surface, therefore the boundary condition for the model is rewritten with R_{cl} being intrinsic thermal resistance of clothing and f_{cl} being a dimensionless clothing area factor [Eq.4], and clothing parameters stored globally in COMSOL.

$$-\lambda \frac{\partial T}{\partial n} = \frac{T_s - T_o}{R_{cl} + \frac{1}{f_{cl} \cdot (h_c + h_r)}} \qquad \text{[Eq.4]}$$

Boundary conditions at the surface assumes that internal heat from conduction to the skin is equal to external outward heat loss by radiation, evaporation, and convection [Eq.3] (Appendix 3).

The active system is modelled from sensors, integrators, and effectors from the Stolwijk model. The sensor system involves thermoreceptors and error signals, located in the hypothalamus and peripheral regions. The integrator system processes the sensor signals, while the effector system then enacts responding commands. Error signals modelled are the temperature differences (℃) from the initial set temperature. The hypothalamus (*hy)* error (e_{hy}) and mean skin (*ms)* error (e_s) are calculated with the equations below.

$$e_{hy} = T_{hy} - T_{hy_0} \qquad \text{[Eq.5]}$$

$$e_s = T_{ms} - T_{ms_0} \qquad \text{[Eq.6]}$$

From these signals, vasodilation (*DI*) [Eq.7] and vasoconstriction (*CS*) [Eq.8] are calculated. Shivering heat production is reliant on the error signals and body fat percentage (BF%). The male and female FETM are modelled with the same shivering equation, as BF% is distinct, producing different shivering heat production rates.

$$DI = 28424 \cdot e_{hy} + 4870 \cdot e_s \qquad \text{[Eq.7]}$$

$$CS = 1.1 \cdot \left(-e_{hy}\right) + 3.3 \cdot (e_s) \qquad \text{[Eq.8]}$$

Sweat rate distribution varies across the body, ranging from 5.6 to 10.4 W·m^{-2}. Total metabolic rate (Q_{tot}) [Eq.9] relies on basal metabolic rate (Q_0), shivering heat production (Q_{SH}) and exercise (Q_{EX}).

$$Q_{tot} = \int Q_0 dV + Q_{SH} + Q_{EX} \qquad \text{[Eq.9]}$$

More information on model development can be found in male and female model publications from Castellani et. al [1, 2].

FETM in these simulations uses Backward Differentiation Formula (BDF) solver to predict the thermoregulatory responses with time-dependent study evaluations for 2.5 hours for each combination of conditions of ambient temperature between 1.7℃ (35 °F) and -42℃ (-45°F) and wind speeds from 5ms^{-1} (11.18mph) to 20ms^{-1} (44.74mph) to compare results to the current WCTI [3]. The time to a freezing risk of 5% (skin temperature of -4.8°C) was computed from these results for regions of the cheek, nose, and 5th finger at metabolic rates of 107W, 357W (light exercise), and 507W (moderate/heavy exercise).

Simulation results were additionally compared to published datasets focused on skin temperature in cold conditions [4, 5]. To simulate these real-life conditions in COMSOL, time-dependent piecewise or step functions were used for dynamic parameters such as ambient temperature, wind speed clothing resistance, and metabolic rate of exercise (T_a, v_{air}, R_{cl}, Q_{EX}). In a stationary (no exercise) study by Gavhed et. al [5], 8 males were preconditioned in -5℃ for 60 minutes, immediately followed by 30 minutes exposed to -10℃ with 5.0 m·s^{-1} wind. This published work will be referred to as Gavhed[1] and was simulated in COMSOL using the male FETM. In an extension to this study, Gavhed et. al looked at the effect of moderate to high metabolic rates, with exercise, on thermal responses at -10℃ and 5.0m·s^{-1} wind with winter clothing worn following preconditioning (2.2 clo) [6]. This study will be referenced as Gavhed[2] and was simulated with the male FETM with the dynamic ambient parameters.

Results and Discussion

WCTI Results

WCTI simulation results confirm the cheek has the longest exposure time until frostbite compared to the nose and finger in both male and females (Figure 4). This effect in the nose and finger is likely due to their smaller diameters, larger exposure areas relative

to mass and increased vasoconstriction in the peripheral regions. Facial cooling with and without exercise heat production is consistent with previous findings in which cheek skin temperatures were influenced and minimal effect was observed in the nose and finger [4] (Figure 5). Nose times to frostbite remained the same with added exercise, while the cheek was impacted largely with exercise at higher temperatures (Figure 6 & 7).

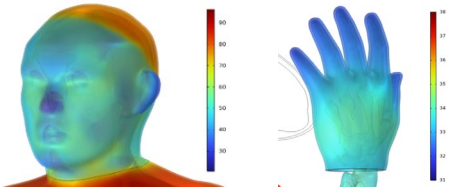

Figure 3: Female FETM face [left] and hand [right] during 0W exercise WCTI simulation.

Figure 5: Male model thermoneutral [left] and simulation at -15C and 15 m/s at no exercise [2nd], 250W exercise [3rd] and 400W exercise [right].

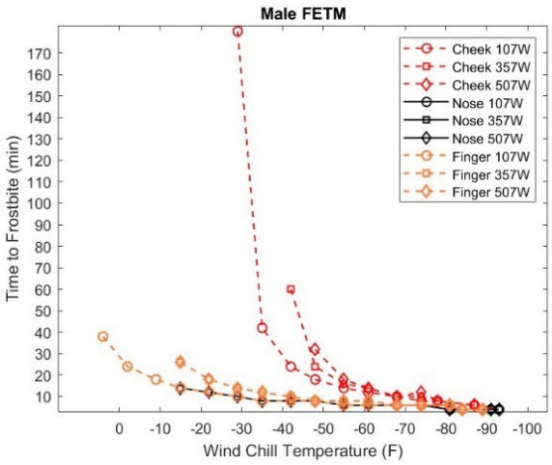

Figure 6: Male FETM WCTI simulations time to frostbite in the cheek [red], nose [black], and finger [orange] at different exercise heat production rates [W].

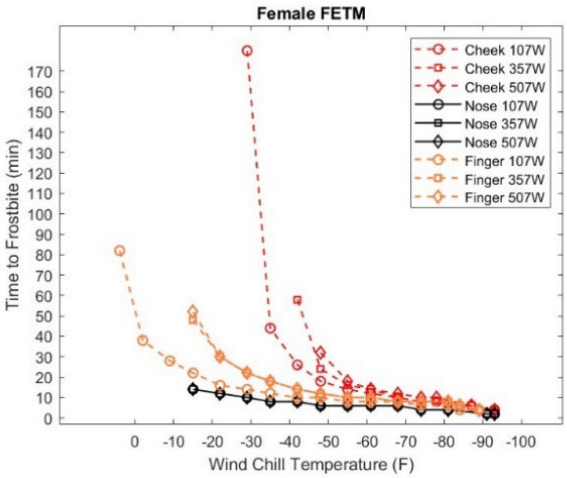

Figure 7: Female FETM WCTI simulations time to frostbite in the cheek [red], nose [black], and finger [orange] at different exercise heat production rates [W].

Between the male and female model, the female nose reached frostbite marginally faster than the male model. Predicted cheek times to frostbite were similar between the two models with and without exercise. However, in the finger, the female model consistently reached frostbite at a slower rate (~2 min less) than the male finger (Figure 8). This effect is possibly due to the higher initial temperature in the finger of the female model compared to the male (0.6℃) higher. Initial temperatures were estimated in each model based on population averages in previous studies.

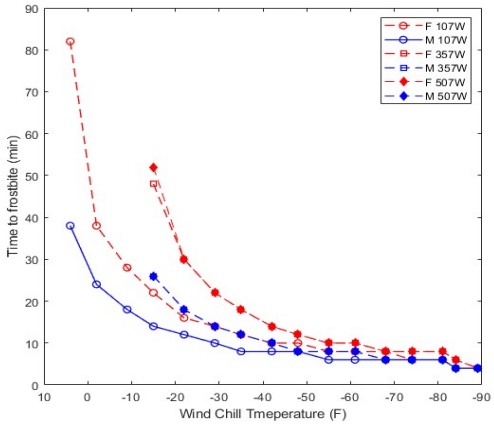

Figure 8: Male FETM [blue] and female FETM [red] finger time to frostbite.

In relation to the NWS 2001 WCTI, the FETM produces considerably longer prediction times to frostbite in the cheek, although, FETM nose frostbite

times are comparable to the 2001 WCTI. Overall, exercise has little impact in extending exposure time to frostbite and reducing frostbite risk as wind chill temperature decreases, specifically in the nose.

Published Dataset Results

The FETM simulation results for Gavhed[1] comparison shows good agreement for the cheek following the "preconditioning" phase (Figure 9). The FETM does not agree well in the preconditioning phase (0-60min), possibly due to initial values or damping effects cause by BDF. Notably, subjects' average initial cheek skin temperatures were much lower than the model's initial temperature [33℃]. Nose skin temperature difference between predicted and observed values were more varied in the "experimental" portion of the study (60-90min), possibly due to unpredictable cold-induced vasodilation responses in the subjects.

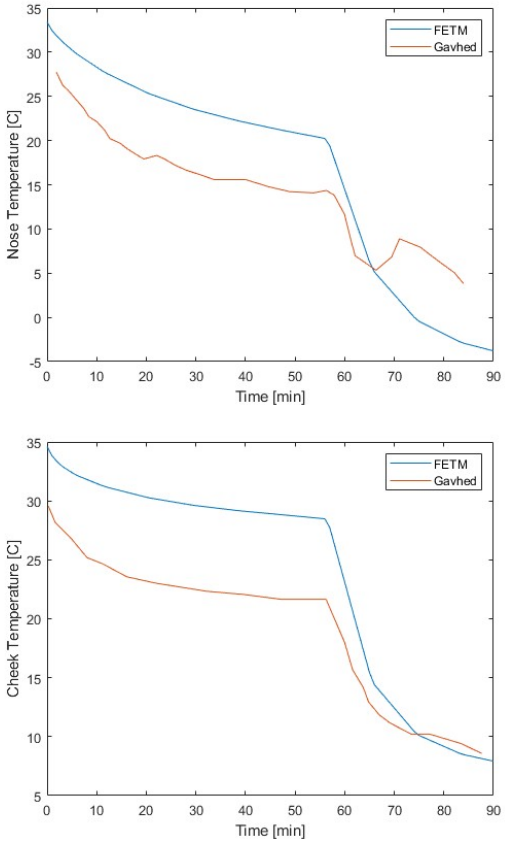

Figure 4: Gavhed[1] observed nose [top] and cheek [bottom] results [blue] compared to male FETM simulation of protocol [orange].

In the exercise study, the average skin temperature is observed during light exercise [LE] and heavy exercise [HE] (Figure 10). Again, the FETM closely corresponds to the observed dataset after preconditioning (after 60min). The average temperatures following LE and HE FETM simulations are 26.4℃ and 27.9℃ at LE and HE. Gavhed[2] final average temperatures observed are 26.1℃ and 27.4℃ at LE and HE, respectively. The model simulation of this dataset shows a similar effect of moderate exercise as the observed results. The FETM overpredicts average skin temperature at HE (moderate exercise) compared to the observed data.

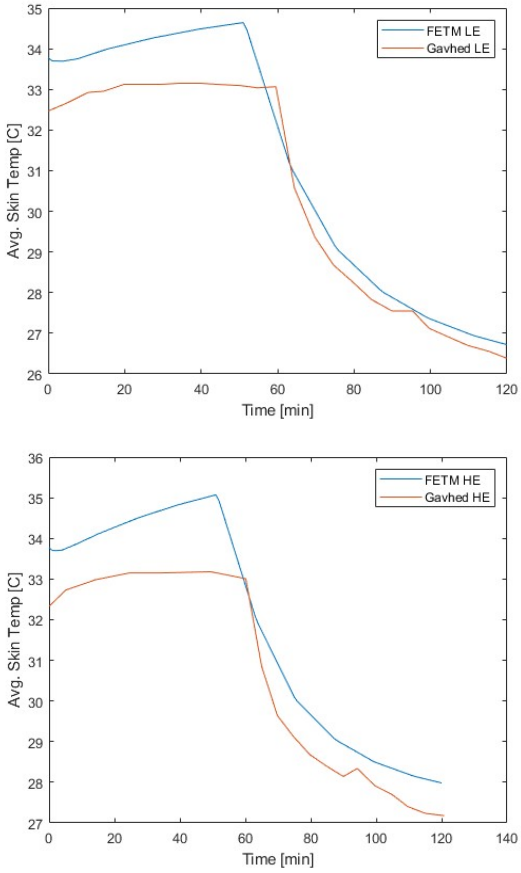

Figure 5: Gavhed[2] observed average skin temperature at moderate exercise – LE [top] and high exercise – HE [bottom] results [orange] compared to male FETM simulation of protocol [blue].

Conclusion

The male and female FETM in COMSOL Multiphysics can be used to estimate human heat transfer and thermoregulation in extreme conditions. The male and female models produce similar results

for spatial temperature distribution. Model differences between sexes are only observed in finger times to frostbite from these results. The current NWS WCTI only considers the cheek frostbite risk at rest. These results suggest that the cheek is not the most susceptible site for frostbite risk. The nose and finger are more susceptible. Results indicate exercise may increase exposure time to frostbite for the cheek, although produces minimal effect in the nose and finger. Exercise has minimal effect on all regions as wind chill temperature decreases. All model results must be further validated with human trials.

References

1. Castellani, M.P.; Rioux T.P.;Castellani, J.W.; Potter, A.W.; Notley, S.R.; Xu, X; *Finite element model of female thermoregulation with geometry based on medical images.* Journal of Thermal Biology, 2023. **113**.
2. Castellani, M.P., Rioux, T.P.; Castellani, J.W.; Potter, A.W.; Notley, S.R.; Xu, X; *A geometrically accurate 3 dimensional model of human thermoregulation for transient cold and hot environments.* Comput Biol Med, 2021. **138**: p. 104892.
3. National Weather Service, *Windchill Temperature Index*, W. Office of Climate, and Weather Services, Editor. 2001, National Oceanic and Atmospheric Administration: Washington, D.C.
4. Gavhed, D.; Makinen, T.; Holmer, I; Rintamaki, H.; *Face cooling by wind in walking subjects.* J Biometeorol, 2003. **47**: p. 7.
5. Gavhed, D.; Makinien, T.; Holmer, I; Rintamaki, H.; *Face temperature and cardiorespiratory responses to wind in thermoneutral and cool subjects exposed to -10C.* J Appl Physiol 2000. **83**: p. 7.
6. Gavhed, D; Makinen, T; Holmer, I; Rintamaki, H, *Effects of metabolic rate on thermal responses at different air velocities in -10 degrees C.* Comp Biochem Physiol A Mol Integr Physiol, 2001. **128**: p. 9

Appendix

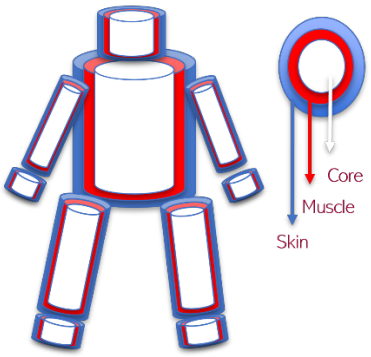

Appendix 1: Cylindrical multi-layered human model.

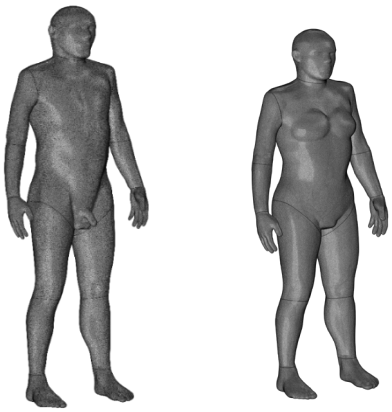

Appendix 2: Male [left] and female [right] mesh creations from XCAT images.

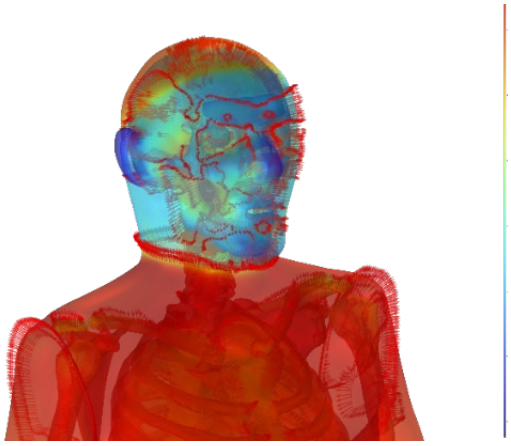

Appendix 3:Heat flux (red arrows) along mesh nodes in male model.

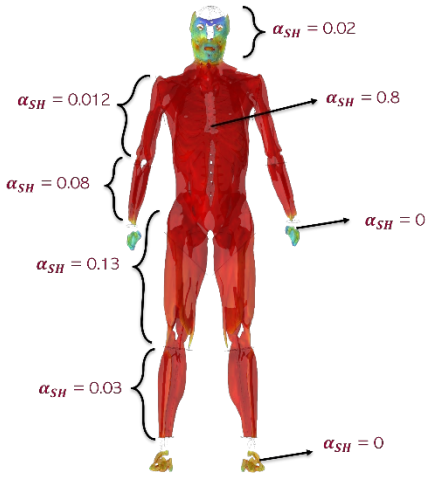

Appendix 4: Shivering metabolic heat production distribution factor.